Atmospheric
Chemistry
and Physics

Supplement of

Global sensitivities of reactive N and S gas and particle concentrations and deposition to precursor emissions reductions

Yao Ge et al.

Correspondence to: Yao Ge (y.ge-7@sms.ed.ac.uk) and Mathew R. Heal (m.heal@ed.ac.uk)

1 Model-measurement comparison for RDN species

The global model evaluation of N_r and S_r concentrations and wet deposition from this model configuration for 2010 and 2015 against measurements from 10 ambient monitoring networks is documented in Ge et al. (2021) and demonstrates the model's capability for capturing the spatial and seasonal variations of NH_3, NH_4^+, NO_2, HNO_3, NO_3^-, SO_2, and SO_4^{2-} in East Asia,
Southeast Asia, Europe, and North America.

Figure S1 gives an example of model-measurement comparisons of 2015 annual average surface concentrations of NH_3 and NH_4^+, and annual wet deposition of reduced N (RDN $= NH_3 + NH_4^+$) in East Asia, Southeast Asia, Europe, and North America. Model and measurements consistently show higher RDN concentrations and wet deposition in East Asia compared to other regions, which is consistent with East Asia becoming a hot spot of RDN pollution in recent years (Szopa et al., 2021; Hoesly
et al., 2018). The modelled annual average NH_3 concentrations show similar agreement with measurements from the four regions, with the correlation coefficient R ranging from 0.56 to 0.72. The linear correlations between modelled and measured NH_4^+ are highest in Southeast Asia, followed by Europe and North America, while East Asia shows a relatively poor correlation, reflecting potential differences among individual measurement networks. For wet deposition of RDN, the model simulates smaller values by 21% - 50% across 5 different networks. Further examination of wet deposition components reveals
that this is largely driven by a general underestimation of annual total precipitation (Ge et al., 2021). Given the localised nature of precipitation events and the intrinsic scale mismatch between a 1° model grid volume average and a single sampling point, such a model underestimation range is expected.

The model-measurement comparison metrics in this work are comparable with other global modelling studies. Hauglustaine et al. (2014) reported that the R values of their global model results (LMDz-INCA global chemistry–aerosol–climate model,
1.9° latitude $\times$ 3.75° longitude resolution) versus measurements in 2006 for surface concentrations of SO_4^{2-}, NH_4^+ and NO_3^- ranged 0.43-0.58 in Europe and 0.54-0.77 in North America, which is similar to our results presented here. The AeroCom phase III global nitrate experiment, which includes 9 models, reported slightly lower R ranges than here for annual NO_3^- in 2008: 0.081-0.735 in North America, 0.393-0.585 in Europe, and 0.226-0.429 in Southeast Asia (Bian et al., 2017). Again, for detailed analyses of evaluation statistics of other species, please refer to our previous model evaluation study Ge et al. (2021).
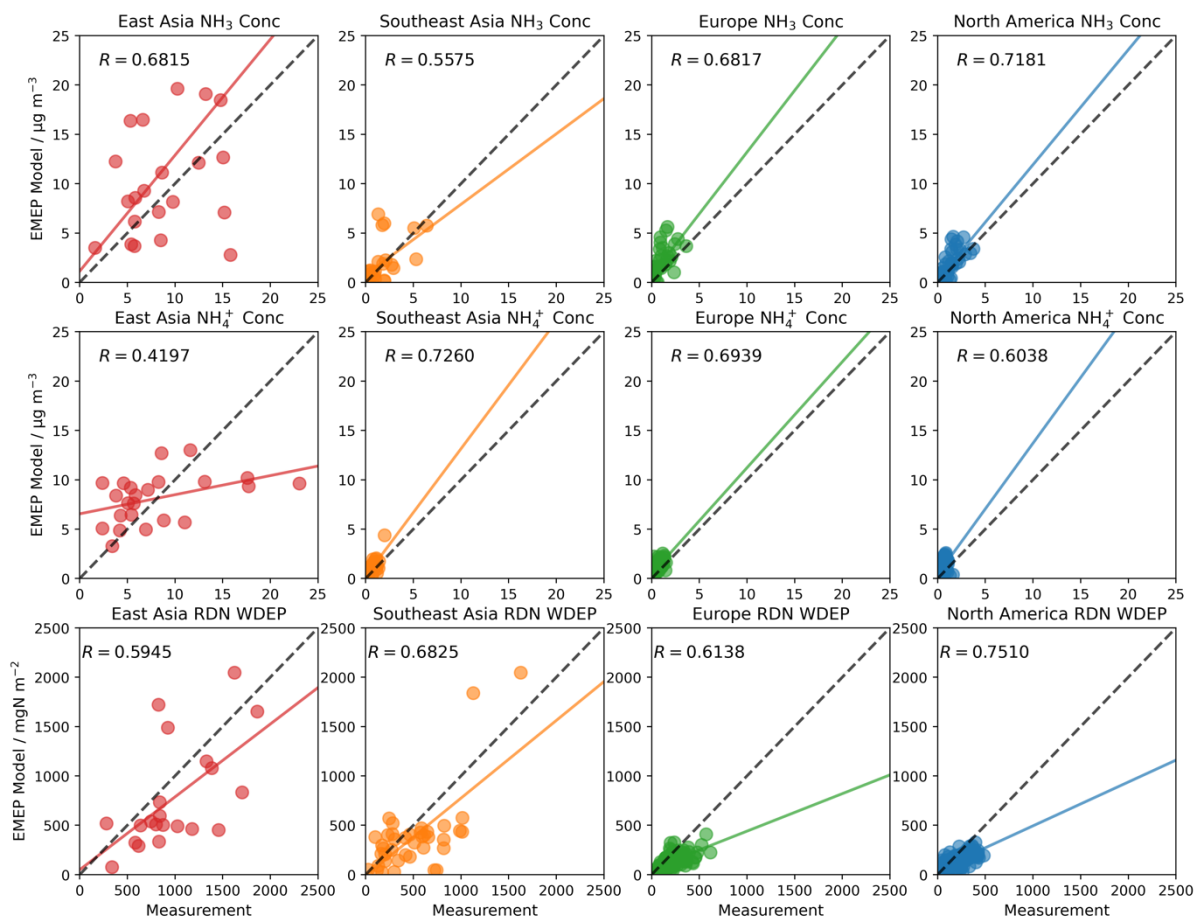
Figure S1. Comparisons of 2015 annual average surface concentrations of NH$_3$ (top row) and NH$_4^+$ (middle row), and annual wet deposition of reduced N (RDN = NH$_3$ + NH$_4^+$; bottom row) between model and measurements in East Asia (Chinese NNDMN network), Southeast Asia (EANET network), Europe (EMEP network) and North America (US EPA and Canadian NAPS networks). In each plot, *R* is the Pearson correlation coefficient, the solid line is the least-squares regression line, and the dashed black line is the 1:1 line. Detailed information about measurement networks is presented in Ge et al. (2021).

Table S1: The allocation of IPCC reference regions (Iturbide et al., 2020) in the 4 world regions used in this study.

| World regions in this paper	IPCC region numbers (0-57)
East Asia	35
South Asia	37
Euro_Medi	16, 17, 19
North America	3, 4, 5

55

Table S2: Global and regional sensitivities of NH$_3$ and NH$_4^+$ surface concentrations to individual emission reductions.
60 **Absolute difference $\left(\text{AD, } \mu g \, m^{-3}\right) = \text{Emission reduction} - \text{Baseline}$.** **Relative difference (RD, %) $= \frac{AD}{\text{Baseline}} \times 100\%$.** **Entries in the table are shaded as follows: light blue represents 'negative difference'; light red represents 'positive difference'; no colour represents negligible differences (i.e., $|RD| \leq 3\%$).**

Scenario	-20% NH$_3$		-20% NO$_x$		-20% SO$_x$		-20% All-3		-40% NH$_3$		-40% NO$_x$		-40% SO$_x$		-40% All-3	
	AD	RD	AD	RD	AD	RD	AD	RD	AD	RD	AD	RD	AD	RD	AD	RD
	NH$_3$															
East Asia	-1.03	-25%	0.10	2%	0.14	3%	-0.82	-20%	-2.04	-49%	0.24	6%	0.28	7%	-1.62	-39%
	NH$_4^+$															
	-0.22	-6%	-0.17	-5%	-0.32	-9%	-0.67	-19%	-0.51	-15%	-0.42	-12%	-0.64	-19%	-1.39	-40%
	NH$_3$															
South Asia	-1.23	-24%	0.04	1%	0.19	4%	-1.01	-19%	-2.47	-47%	0.09	2%	0.38	7%	-2.02	-39%
	NH$_4^+$															
	-0.05	-2%	-0.10	-4%	-0.42	-17%	-0.54	-22%	-0.11	-4%	-0.21	-8%	-0.85	-34%	-1.07	-43%
	NH$_3$															
Euro_Medi	-0.27	-25%	0.03	2%	0.05	4%	-0.21	-19%	-0.53	-49%	0.06	5%	0.10	9%	-0.42	-38%
	NH$_4^+$															
	-0.08	-8%	-0.06	-6%	-0.10	-10%	-0.22	-22%	-0.18	-18%	-0.14	-13%	-0.21	-20%	-0.44	-43%
	NH$_3$															
North America	-0.24	-24%	0.03	3%	0.03	3%	-0.19	-19%	-0.48	-48%	0.06	6%	0.06	6%	-0.38	-38%
	NH$_4^+$															
	-0.03	-5%	-0.06	-8%	-0.07	-11%	-0.15	-23%	-0.08	-12%	-0.12	-18%	-0.14	-22%	-0.30	-46%
	NH$_3$															
Globe	-0.09	-24%	0.00	1%	0.02	4%	-0.07	-19%	-0.17	-48%	0.01	3%	0.03	9%	-0.13	-38%
	NH$_4^+$															
	-0.02	-6%	-0.01	-4%	-0.04	-13%	-0.06	-21%	-0.04	-14%	-0.02	-8%	-0.08	-28%	-0.12	-42%
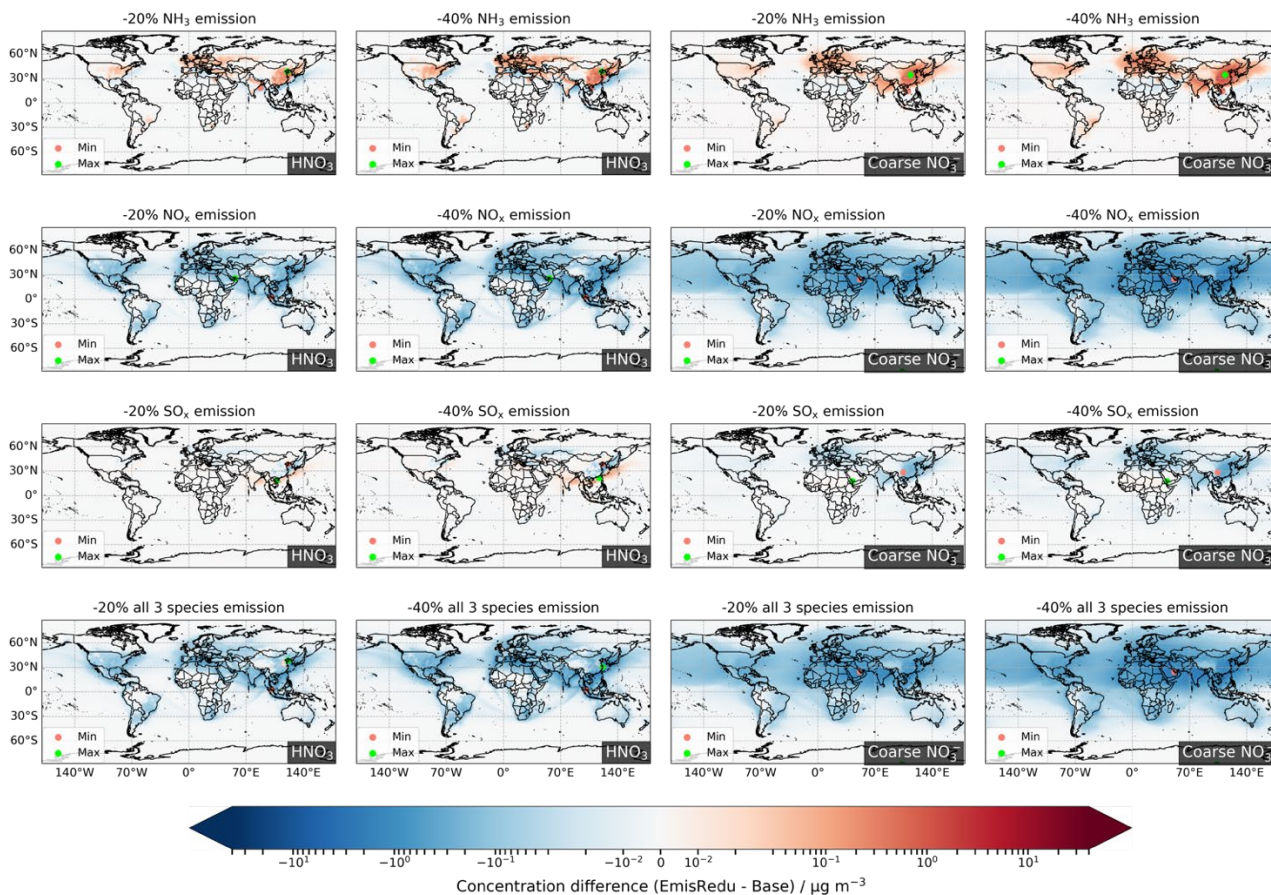
Figure S2: Changes in HNO₃ and coarse NO₃⁻ annual surface concentrations for 20% and 40% emissions reductions in NH₃, NOₓ, and SOₓ individually and collectively. Red and green dots in each map locate the minimum and maximum difference, respectively.
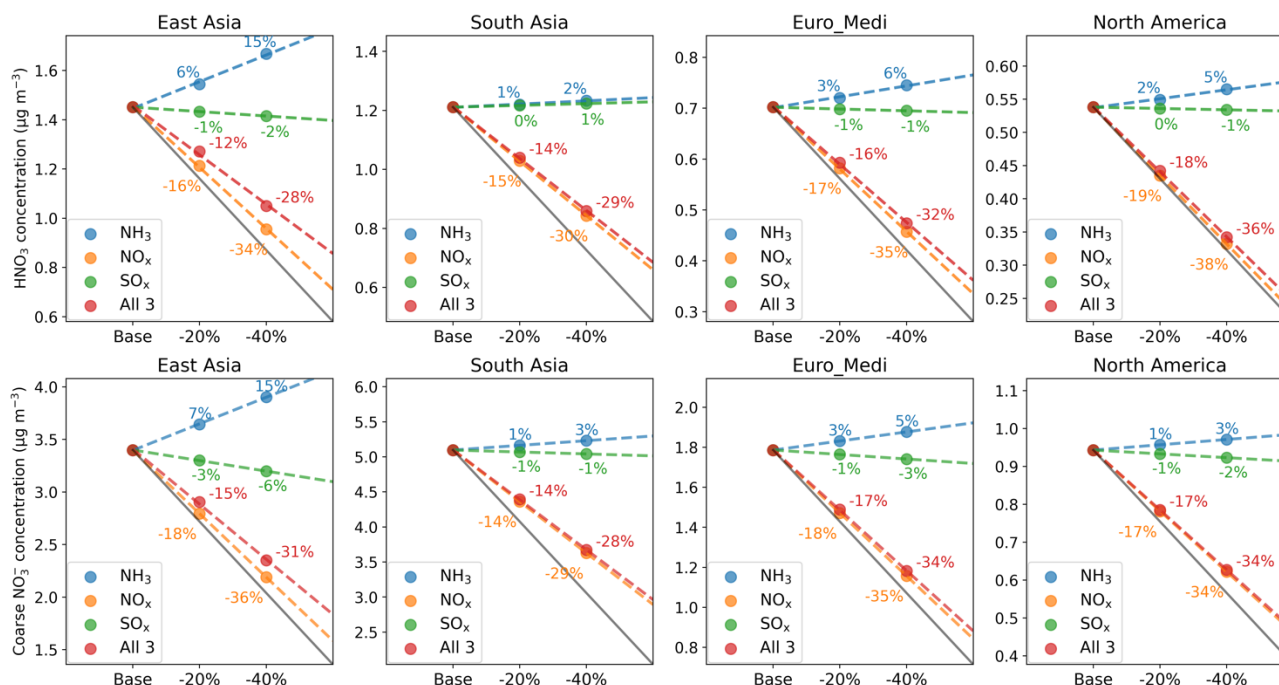
Figure S3: The absolute and relative sensitivities of regionally-averaged annual mean surface concentrations of HNO₃ (upper row) and coarse NO₃⁻ (lower row) to 20% and 40% emissions reductions in NH₃ (blue), NOₓ (orange) and SOₓ (green) individually, and collectively (red), for the four regions defined in Fig. 1. The solid grey line in each panel illustrates the one-to-one relative response to emissions reductions, whilst the coloured dashed lines are the linear regressions through each set of three model simulations and illustrate the actual responses to emissions reductions of a given precursor. The numbers show the corresponding relative responses to each emissions reduction (with respect to baseline).

5

Table S3: Global and regional sensitivities of NO_x, HNO_3, fine NO_3^- and coarse NO_3^- surface concentrations to individual emission reductions. Absolute difference $(AD, \ \mu g \, m^{-3})$ = Emission reduction − Baseline. Relative difference (RD, %) = $\frac{AD}{Baseline} \times 100\%$. Entries in the table are shaded as follows: light blue represents 'negative difference'; light red represents 'positive difference'; no colour represents negligible differences (i.e., $|RD| \leq 3\%$).

Scenario	-20% NH₃		-20% NOₓ		-20% SOₓ		-20% All-3		-40% NH₃		-40% NOₓ		-40% SOₓ		-40% All-3	
	AD	RD	AD	RD	AD	RD	AD	RD	AD	RD	AD	RD	AD	RD	AD	RD
East Asia — NOₓ	-0.03	-0%	-2.54	-24%	0.00	0%	-2.57	-24%	-0.08	-1%	-4.76	-45%	0.01	0%	-4.79	-45%
HNO₃	0.09	6%	-0.24	-16%	-0.02	-1%	-0.18	-12%	0.22	15%	-0.50	-34%	-0.04	-2%	-0.40	-28%
Fine NO₃⁻	-0.72	-14%	-0.72	-14%	0.20	4%	-1.10	-22%	-1.62	-32%	-1.65	-33%	0.40	8%	-2.26	-45%
Coarse NO₃⁻	0.25	7%	-0.60	-18%	-0.10	-3%	-0.49	-15%	0.51	15%	-1.21	-36%	-0.20	-6%	-1.05	-31%
South Asia — NOₓ	-0.00	-0%	-0.80	-11%	-0.01	0%	-0.81	-11%	-0.01	-0%	-1.57	-22%	-0.02	-0%	-1.59	-23%
HNO₃	0.01	1%	-0.18	-15%	0.01	0%	-0.17	-14%	0.02	2%	-0.37	-30%	0.01	1%	-0.35	-29%
Fine NO₃⁻	-0.15	-18%	-0.19	-23%	0.03	4%	-0.28	-33%	-0.33	-39%	-0.38	-45%	0.07	8%	-0.51	-60%
Coarse NO₃⁻	0.07	1%	-0.73	-14%	-0.03	-1%	-0.70	-14%	0.13	3%	-1.47	-29%	-0.06	-1%	-1.42	-28%
Euro_Medi — NOₓ	-0.00	-0%	-0.80	-20%	0.00	0%	-0.80	-20%	-0.01	-0%	-1.55	-38%	0.01	0%	-1.55	-38%
HNO₃	0.02	3%	-0.12	-17%	-0.00	0%	-0.11	-15%	0.04	6%	-0.24	-35%	-0.01	-1%	-0.23	-32%
Fine NO₃⁻	-0.17	-15%	-0.22	-19%	0.04	4%	-0.31	-27%	-0.37	-33%	-0.47	-41%	0.09	8%	-0.61	-53%
Coarse NO₃⁻	0.04	3%	-0.32	-18%	-0.02	-1%	-0.30	-17%	0.09	5%	-0.63	-35%	-0.05	-3%	-0.60	-34%
North America — NOₓ	-0.00	-0%	-0.75	-19%	0.00	0%	-0.75	-18%	-0.01	-0%	-1.47	-36%	0.01	0%	-1.47	-36%
HNO₃	0.01	2%	-0.10	-19%	-0.00	0%	-0.10	-18%	0.03	5%	-0.21	-38%	-0.00	-1%	-0.20	-36%
Fine NO₃⁻	-0.10	-12%	-0.18	-20%	0.02	2%	-0.24	-27%	-0.23	-26%	-0.37	-42%	0.04	4%	-0.46	-53%
Coarse NO₃⁻	0.01	2%	-0.16	-17%	-0.01	-1%	-0.16	-17%	0.03	3%	-0.32	-34%	-0.02	-2%	-0.32	-34%
Globe — NOₓ	-0.00	-0%	-0.16	-15%	0.00	0%	-0.16	-15%	-0.00	-0%	-0.31	-30%	0.00	0%	-0.31	-30%
HNO₃	0.00	1%	-0.03	-15%	-0.00	0%	-0.03	-15%	0.01	3%	-0.06	-31%	-0.00	-1%	-0.05	-30%
Fine NO₃⁻	-0.03	-14%	-0.03	-16%	0.01	5%	-0.05	-22%	-0.06	-30%	-0.07	-35%	0.02	10%	-0.09	-44%
Coarse NO₃⁻	0.01	1%	-0.10	-14%	-0.01	-1%	-0.10	-14%	0.02	2%	-0.21	-28%	-0.01	-2%	-0.21	-28%

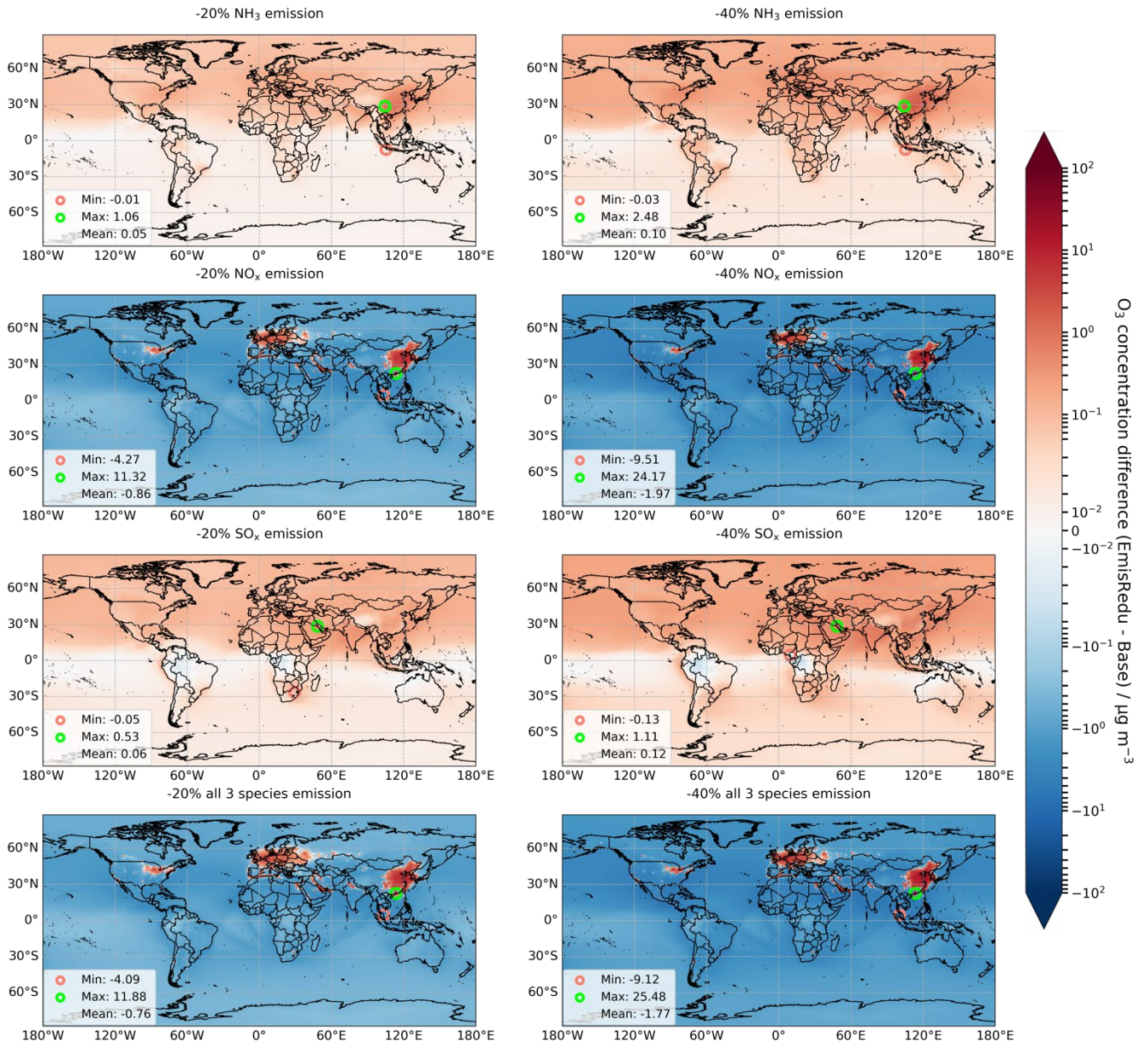**Figure S4:Changes in O₃ annual surface concentrations for 20% and 40% emissions reductions in NH₃, NOₓ, and SOₓ individually and collectively. Red and green dots in each map locate the minimum and maximum difference, respectively.**

85

90

95

Table S4: Global and regional sensitivities of SO₂, and SO₄²⁻ surface concentrations to individual emission reductions. Absolute difference $\left(\text{AD, } \mu g\ m^{-3}\right) = $ Emission reduction − Baseline.   Relative difference $\left(\text{RD, \%}\right) = \frac{AD}{\text{Baseline}} \times 100\%$. Entries in the table are shaded as follows: light blue represents 'negative difference'; light red represents 'positive difference'; no colour represents negligible differences (i.e., $|RD| \leq 3\%$).

Scenario	-20% NH₃		-20% NOₓ		-20% SOₓ		-20% All-3		-40% NH₃		-40% NOₓ		-40% SOₓ		-40% All-3	
	AD	RD	AD	RD	AD	RD	AD	RD	AD	RD	AD	RD	AD	RD	AD	RD
East Asia — SO₂	0.31	7%	-0.10	-2%	-1.01	-24%	-0.87	-20%	0.71	16%	-0.21	-5%	-1.95	-45%	-1.75	-41%
East Asia — SO₄²⁻	0.02	0%	0.10	2%	-1.06	-19%	-0.97	-17%	0.07	1%	0.17	3%	-2.12	-38%	-2.01	-36%
South Asia — SO₂	0.10	4%	0.02	1%	-0.52	-22%	-0.46	-19%	0.34	14%	0.05	2%	-1.01	-43%	-0.92	-39%
South Asia — SO₄²⁻	0.05	1%	-0.11	-2%	-1.18	-19%	-1.25	-20%	0.14	2%	-0.27	-4%	-2.37	-38%	-2.50	-41%
Euro_Medi — SO₂	0.05	4%	-0.01	-1%	-0.26	-22%	-0.23	-19%	0.12	10%	-0.01	-1%	-0.50	-42%	-0.45	-38%
Euro_Medi — SO₄²⁻	-0.00	-0%	0.00	0%	-0.36	-17%	-0.36	-17%	-0.00	-0%	-0.01	-1%	-0.72	-34%	-0.73	-35%
North America — SO₂	0.03	5%	-0.00	-1%	-0.12	-22%	-0.10	-20%	0.07	14%	-0.01	-1%	-0.23	-43%	-0.20	-39%
North America — SO₄²⁻	0.00	0%	-0.01	-1%	-0.22	-19%	-0.23	-19%	0.01	1%	-0.03	-3%	-0.44	-37%	-0.46	-39%
Globe — SO₂	0.01	3%	-0.00	-0%	-0.07	-19%	-0.06	-17%	0.03	8%	-0.00	-0%	-0.13	-36%	-0.12	-33%
Globe — SO₄²⁻	0.00	0%	-0.00	-1%	-0.14	-16%	-0.14	-17%	0.01	1%	-0.01	-2%	-0.29	-33%	-0.29	-34%
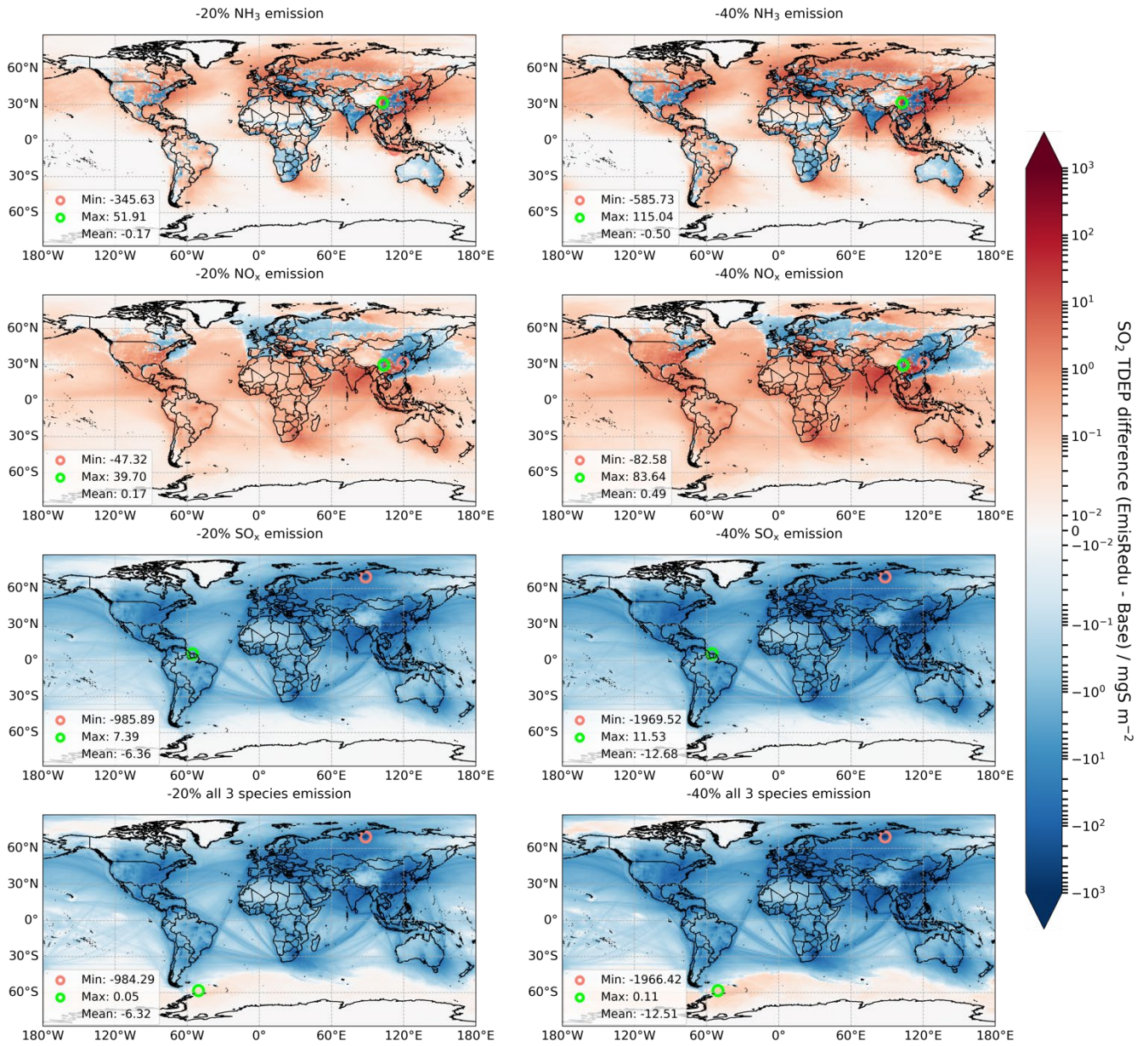
Figure S5: Changes in SO₂ total deposition (wet + dry; abbreviated as TDEP) for 20% and 40% emissions reductions in NH₃, NOₓ, and SOₓ individually and collectively. Red and green dots in each map locate the minimum and maximum difference, respectively.
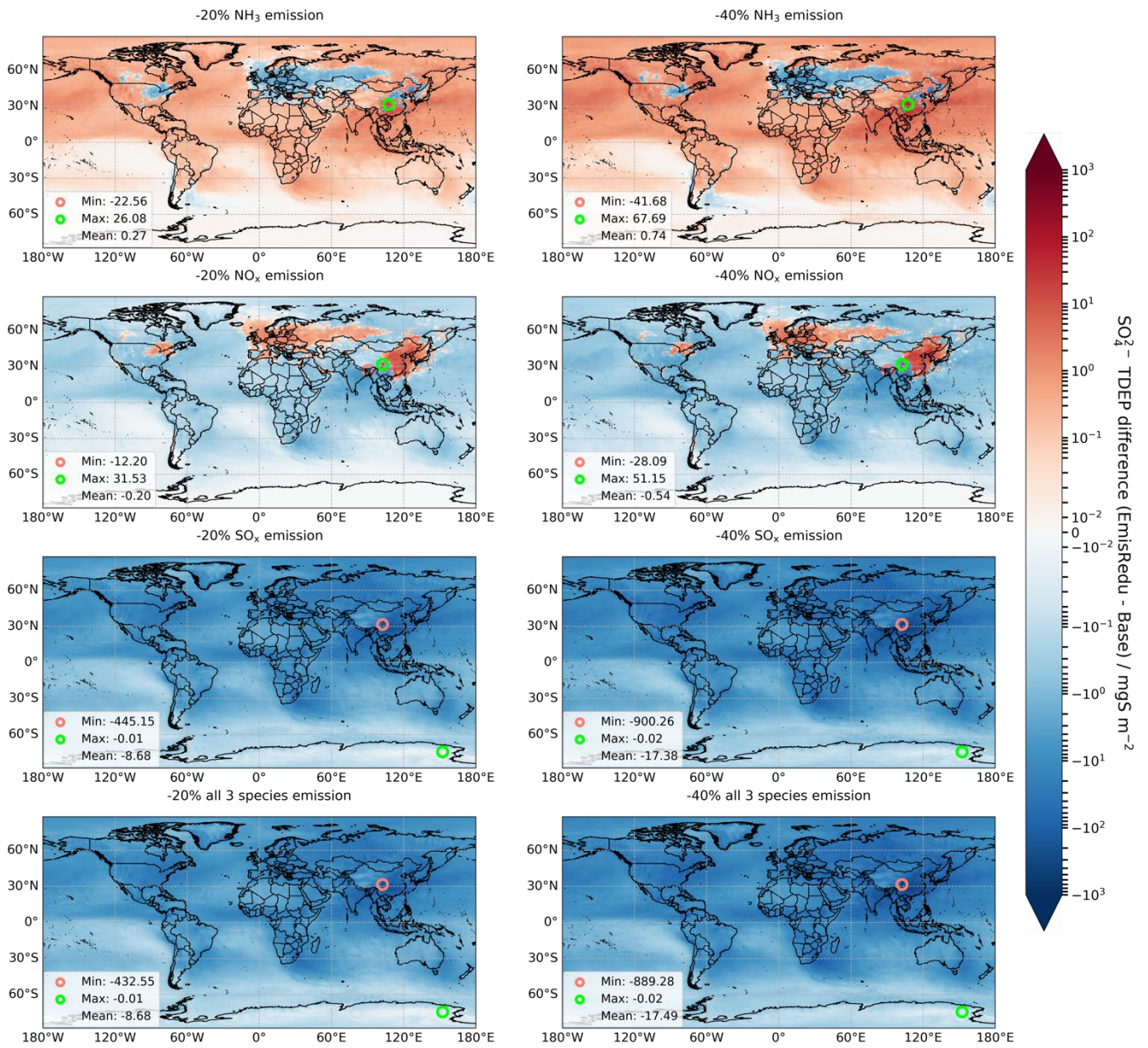
Figure S6: Changes in SO$_4^{2-}$ total deposition (wet + dry; abbreviated as TDEP) for 20% and 40% emissions reductions in NH$_3$, NO$_x$, and SO$_x$ individually and collectively. Red and green dots in each map locate the minimum and maximum difference, respectively.
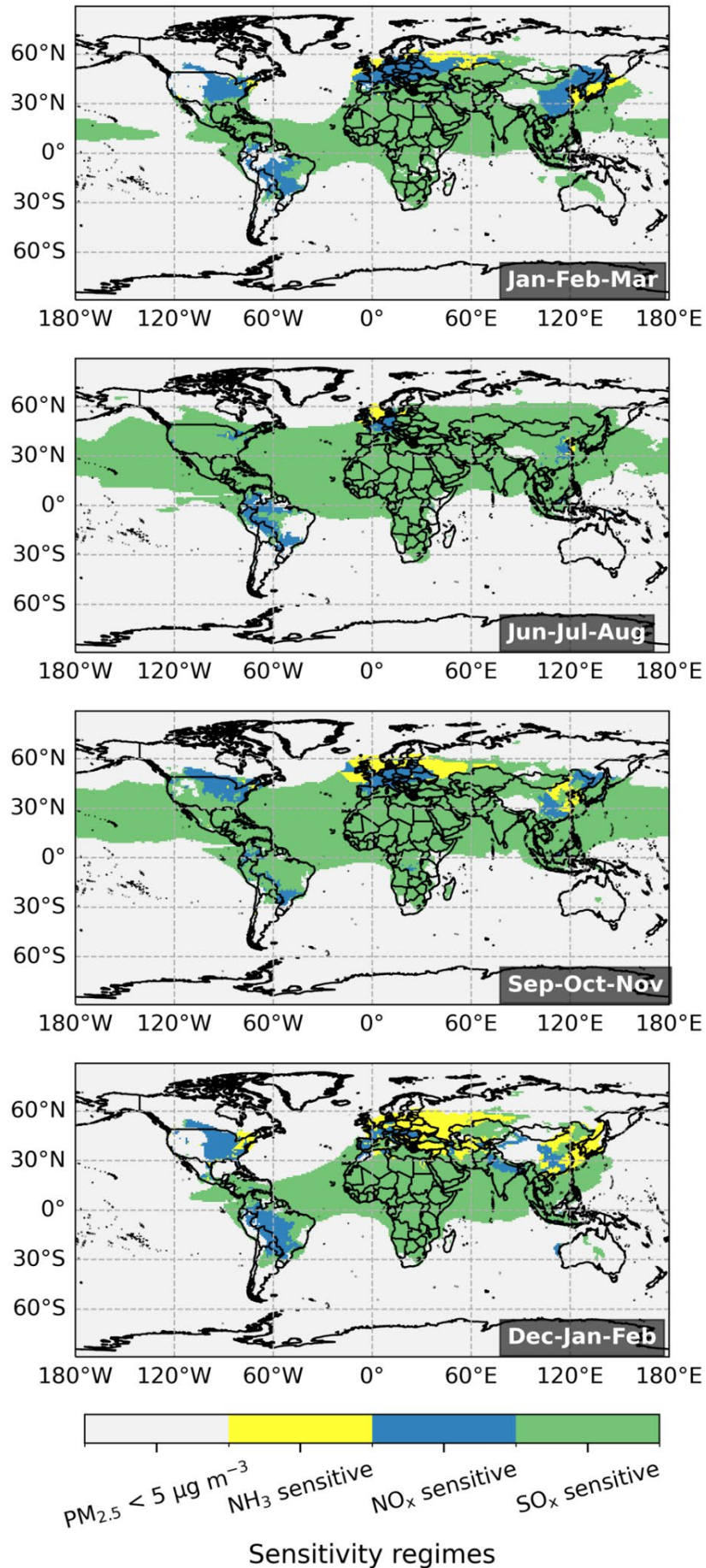
2 Seasonal variations in global PM$_{2.5}$ sensitivity regimes

To reveal more details of temporal variations in global PM$_{2.5}$ sensitivity regimes, we compare PM$_{2.5}$ sensitivities to individual emissions reductions on a seasonal basis using the Northern Hemisphere calendar: spring (March, April, and May), summer (June, July, and August), autumn (September, October, and November), and winter (December, January, and February).

Figure S7 presents the spatial distribution of dominant PM$_{2.5}$ sensitivity regimes in four seasons. In East Asia, the dominant regime shifts from NO$_x$-sensitive to SO$_x$-sensitive from spring to summer, while the NH$_3$-sensitive regime expands more and more from autumn to winter. Similar trends are observed across Europe as well, where NO$_x$-sensitive grids are prevalent during spring while NH$_3$-sensitive grids dominate during winter. The springtime NO$_x$-sensitive regime in these regions can be attributed to large NH$_3$ emissions from intensive agricultural activities in this season (Cheng et al., 2021; Dammers et al., 2019), which leads to the formation of NH$_4$NO$_3$ being primarily limited by the availability of HNO$_3$. Consequently, reductions in NO$_x$ emissions decrease gaseous HNO$_3$ production which then decrease SIA concentrations. In the summer, NH$_4$NO$_3$ becomes less stable due to the generally higher temperature and sulfate aerosols remain a significant contributor to PM$_{2.5}$ in East Asia (Ianniello et al., 2011; Wang et al., 2013). Since the production of sulfate aerosols depends on the oxidation processes of SO$_2$ rather than the availability of NH$_3$, and NH$_3$ is in excess anyway, SO$_x$ emissions reductions become the most effective single-precursor control for PM$_{2.5}$ mitigation in this region. The wintertime NH$_3$-sensitive regime in both Europe and East Asia is caused by smaller NH$_3$ emissions (due to reduced agricultural activities) and relatively larger NO$_x$ emissions (such as from increased domestic heating). Changes in meteorological factors (e.g., decreased vertical dispersion) may also contribute to higher NO$_x$ surface concentrations in the winter. As a result, NH$_3$ becomes the limiting factor in NH$_4$NO$_3$ formation and therefore has the greatest impact on PM$_{2.5}$ sensitivities.

In contrast, North America and South Asia do not show significant seasonal variations in PM$_{2.5}$ sensitivity regimes. In the eastern US, PM$_{2.5}$ formation is NO$_x$-sensitive for most of the year, except for the summer when it is SO$_x$ sensitive. This suggests that further reductions in NO$_x$ emissions are necessary to decrease annual PM$_{2.5}$ levels in this region. In South Asia, the SO$_x$-sensitive regime dominates throughout the year, with the exception of northern India in the winter, which is more NO$_x$-sensitive. As discussed in the main paper, the extreme NH$_3$-richness and dominant contribution of sulfate aerosols to SIA in South Asia render PM$_{2.5}$ formation almost exclusively sensitive to SO$_x$ emission reductions.

Figure S7: Spatial and seasonal variation in sensitivity regime of PM$_{2.5}$ mitigation based on data from 40% individual reductions in emissions of NH$_3$, NO$_x$, or SO$_x$. The regime is defined according to the precursor that yields the greatest decreases in grid seasonal average PM$_{2.5}$ concentration: NH$_3$ sensitive (yellow), NO$_x$ sensitive (blue), SO$_x$ sensitive (green). Model grids with baseline seasonal mean PM$_{2.5}$ concentrations <5 μg m^{-3} are masked out.

Table S5: Global and regional sensitivities of PM$_{2.5}$ surface concentrations to individual emission reductions. Absolute difference $\left(\text{AD, } \mu\text{g m}^{-3}\right) = \text{Emission reduction} - \text{Baseline}$. Relative difference $(\text{RD, \%}) = \frac{\text{AD}}{\text{Baseline}} \times 100\%$. Entries in the table are shaded as follows: light blue represents 'negative difference'; light red represents 'positive difference'; no colour represents negligible differences (i.e., $|RD| \leq 3\%$).

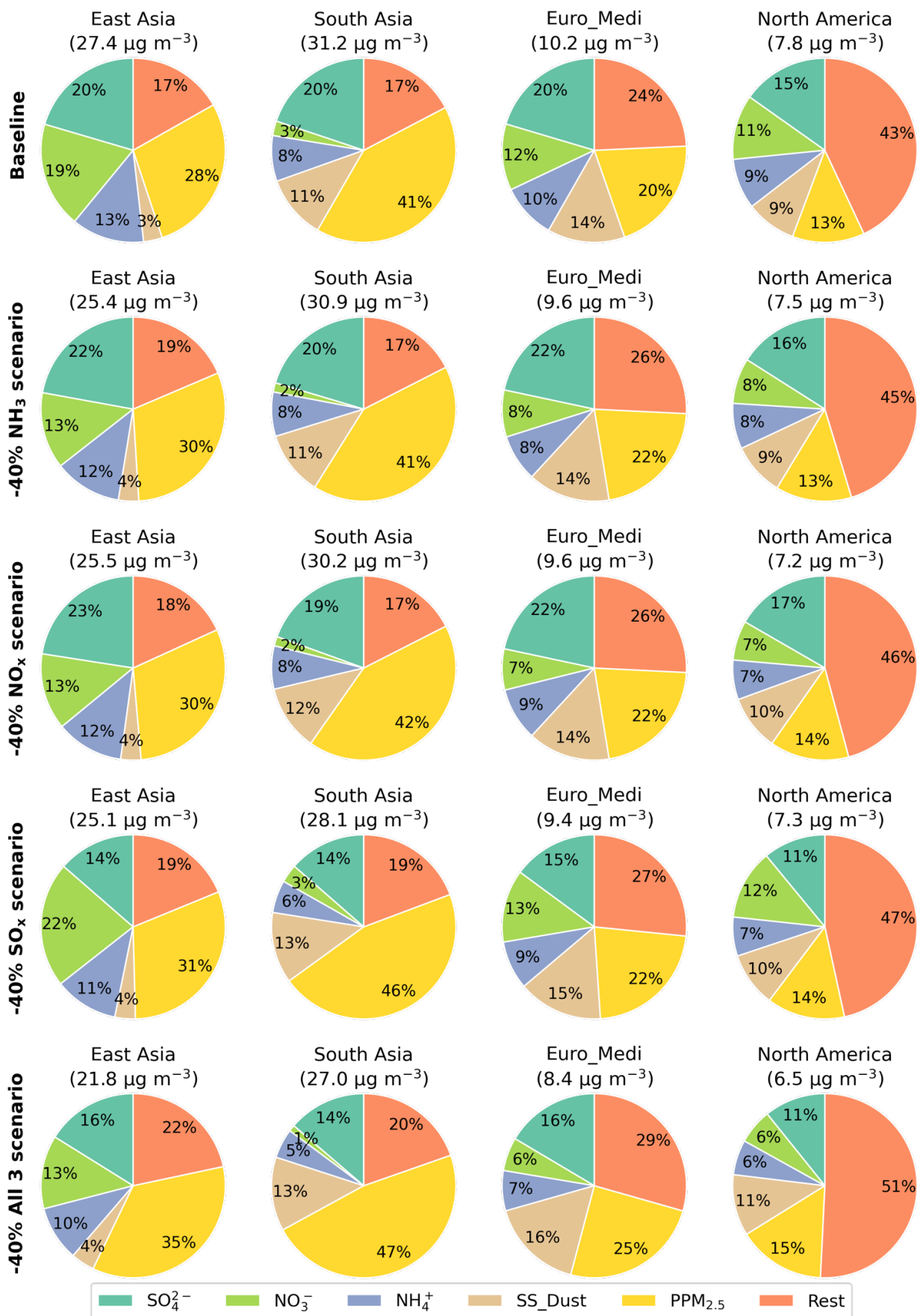| Scenario	-20% NH$_3$		-20% NO$_x$		-20% SO$_x$		-20% All-3		-40% NH$_3$		-40% NO$_x$		-40% SO$_x$		-40% All-3	
PM$_{2.5}$	AD	RD	AD	RD	AD	RD	AD	RD	AD	RD	AD	RD	AD	RD	AD	RD
East Asia	-0.90	-3%	-0.77	-3%	-1.15	-4%	-2.70	-10%	-2.03	-7%	-1.89	-7%	-2.33	-8%	-5.59	-20%
South Asia	-0.15	0%	-0.45	-1%	-1.54	-5%	-2.09	-7%	-0.29	-1%	-0.97	-3%	-3.10	-10%	-4.13	-13%
Euro_Medi	-0.25	-2%	-0.28	-3%	-0.41	-4%	-0.89	-9%	-0.55	-5%	-0.62	-6%	-0.82	-8%	-1.78	-17%
North America	-0.13	-2%	-0.29	-4%	-0.27	-3%	-0.65	-8%	-0.29	-4%	-0.63	-8%	-0.54	-7%	-1.31	-17%
Globe	-0.04	-1%	-0.05	-1%	-0.17	-3%	-0.25	-4%	-0.09	-1%	-0.12	-2%	-0.34	-5%	-0.51	-8%

Figure S8: The percentage contributions of individual PM$_{2.5}$ components to regionally-averaged annual mean surface concentrations of PM$_{2.5}$ in baseline (top row) and scenarios of 40% emissions reductions in NH$_3$ (2nd row), NO$_x$ (3rd row), and SO$_x$ (4th row) individually, and collectively (bottom row), for the four regions defined in Fig. 1. The numbers labelled below each region show the corresponding absolute PM$_{2.5}$ concentrations .

165 **Table S6: The percentage contributions of individual species total deposition (wet + dry) to RDN (NH₃ + NH₄⁺) and OXN (NOₓ + HNO₃ + TNO₃⁻ (fine and coarse NO₃⁻) + Rest OXN) total deposition (TgN yr⁻¹), in baseline and scenarios of 20% and 40% emissions reductions in NH₃, NOₓ, and SOₓ individually and collectively, for the four regions defined in Fig. 1.**

		Baseline	-20% NH₃	-20% NOₓ	-20% SOₓ	-20% All 3	-40% NH₃	-40% NOₓ	-40% SOₓ	-40% All 3
East Asia	RDN	12.0	9.66	12.0	12.0	9.69	7.30	12.1	12.1	7.34
	NH₃	59%	54%	61%	61%	59%	47%	64%	65%	61%
	NH₄⁺	41%	46%	39%	39%	41%	53%	36%	35%	39%
	OXN	8.33	8.36	6.87	8.32	6.88	8.39	5.40	8.31	5.42
	NOₓ	12%	11%	11%	12%	11%	11%	11%	12%	11%
	HNO₃	30%	33%	29%	28%	31%	37%	29%	27%	32%
	TNO₃⁻	54%	51%	54%	55%	53%	47%	54%	57%	51%
	Rest	4%	5%	6%	5%	5%	5%	6%	4%	6%
South Asia	RDN	5.46	4.34	5.47	5.50	4.39	3.22	5.48	5.55	3.32
	NH₃	76%	71%	77%	80%	77%	64%	78%	84%	77%
	NH₄⁺	24%	29%	23%	20%	23%	36%	22%	16%	23%
	OXN	3.08	3.09	2.68	3.08	2.69	3.09	2.28	3.08	2.29
	NOₓ	12%	12%	13%	12%	12%	12%	13%	12%	12%
	HNO₃	29%	30%	29%	29%	29%	30%	29%	29%	29%
	TNO₃⁻	54%	53%	53%	54%	53%	53%	53%	54%	53%
	Rest	5%	5%	5%	5%	6%	5%	5%	5%	6%
Euro_Medi	RDN	3.76	2.99	3.77	3.78	3.02	2.23	3.79	3.80	2.28
	NH₃	64%	60%	67%	67%	66%	55%	69%	70%	67%
	NH₄⁺	36%	40%	33%	33%	34%	45%	31%	30%	33%
	OXN	4.01	4.02	3.29	4.00	3.30	4.04	2.57	4.00	2.58
	NOₓ	14%	14%	14%	14%	14%	14%	14%	14%	14%
	HNO₃	31%	33%	31%	31%	32%	34%	31%	31%	33%
	TNO₃⁻	48%	47%	48%	48%	47%	45%	47%	49%	45%
	Rest	7%	6%	7%	7%	7%	7%	8%	6%	8%
North America	RDN	3.25	2.61	3.26	3.25	2.62	1.98	3.26	3.26	1.99
	NH₃	61%	57%	63%	65%	63%	51%	66%	68%	64%
	NH₄⁺	39%	43%	37%	35%	37%	49%	34%	32%	36%
	OXN	3.73	3.74	3.08	3.73	3.08	3.75	2.43	3.72	2.44
	NOₓ	15%	15%	15%	15%	15%	15%	15%	15%	15%
	HNO₃	38%	39%	36%	36%	37%	41%	35%	35%	36%
	TNO₃⁻	38%	36%	38%	39%	37%	34%	38%	40%	36%
	Rest	9%	10%	11%	10%	11%	10%	12%	10%	13%

170

Table S7: The percentage contributions of SO$_2$ and SO$_4^{2-}$ total deposition (wet + dry) to OXS total deposition (TgN yr^{-1}), in baseline and scenarios of 20% and 40% emissions reductions in NH$_3$, NO$_x$, and SO$_x$ individually and collectively, for the four regions defined in Fig. 1.

		Baseline	-20% NH$_3$	-20% NO$_x$	-20% SO$_x$	-20% All 3	-40% NH$_3$	-40% NO$_x$	-40% SO$_x$	-40% All 3
East Asia	OXS	8.30	8.28	8.30	6.68	6.66	8.24	8.31	5.06	5.04
	SO$_2$	56%	56%	56%	56%	56%	55%	56%	56%	55%
	SO$_4^{2-}$	44%	44%	44%	44%	44%	45%	44%	44%	45%
South Asia	OXS	2.78	2.77	2.79	2.25	2.25	2.73	2.80	1.71	1.71
	SO$_2$	49%	49%	50%	49%	50%	48%	51%	49%	50%
	SO$_4^{2-}$	51%	51%	50%	51%	50%	52%	49%	51%	50%
Euro_Medi	OXS	3.51	3.49	3.52	2.93	2.92	3.48	3.52	2.34	2.33
	SO$_2$	58%	58%	58%	58%	58%	58%	58%	57%	57%
	SO$_4^{2-}$	42%	42%	42%	42%	42%	42%	42%	43%	43%
North America	OXS	2.12	2.13	2.13	1.74	1.73	2.12	2.13	1.34	1.33
	SO$_2$	44%	44%	45%	44%	45%	43%	45%	44%	44%
	SO$_4^{2-}$	56%	56%	55%	56%	55%	57%	55%	56%	56%
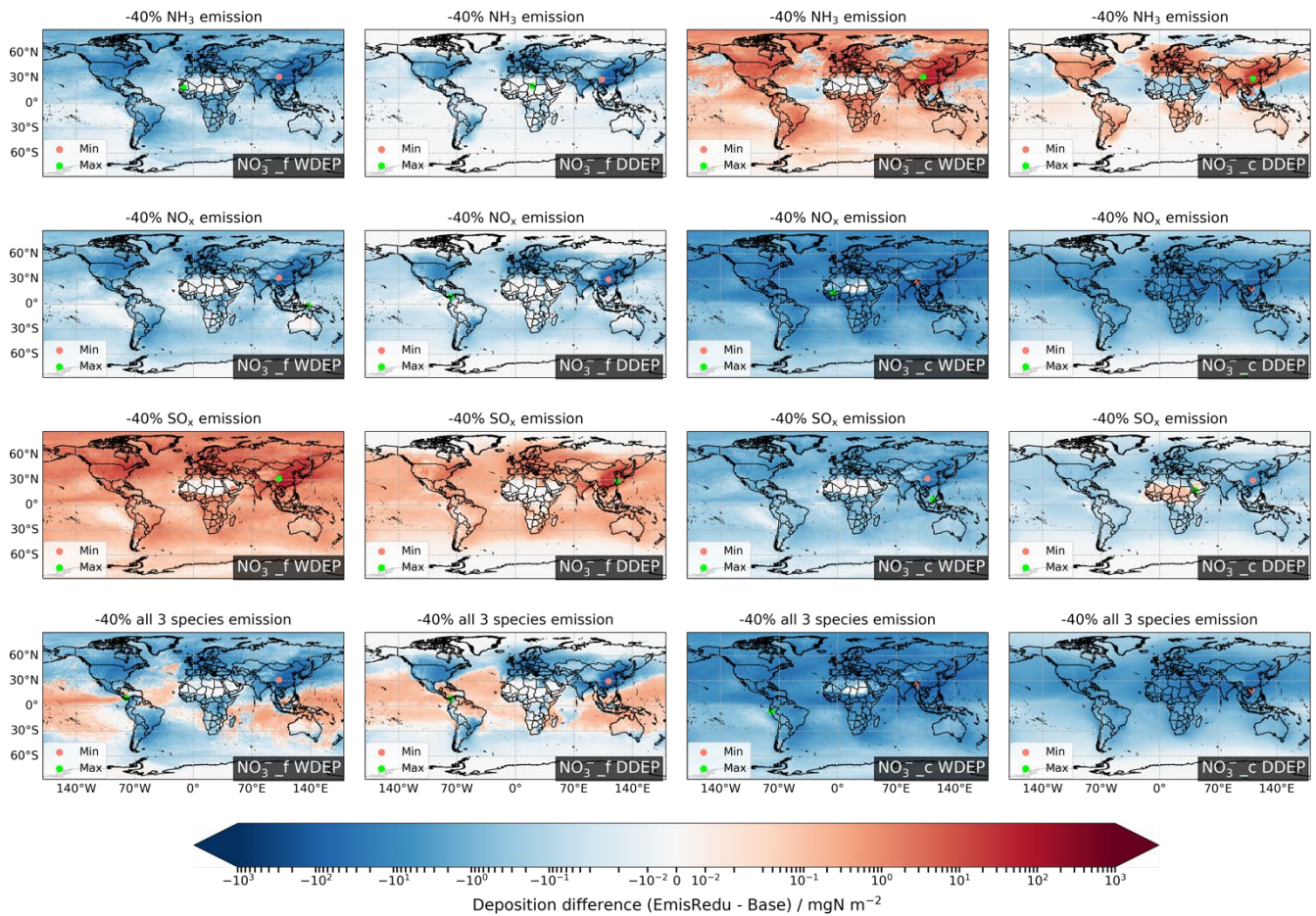
Figure S9: Changes in wet (WDEP) and dry deposition (DDEP) of fine (NO$_3^-$_f) and coarse NO$_3^-$ (NO$_3^-$_c) for 40% emissions reductions in NH$_3$, NO$_x$, and SO$_x$ individually and collectively. Red and green dots in each map locate the minimum and maximum difference, respectively.

185 **References**

Bian, H., Chin, M., Hauglustaine, D. A., Schulz, M., Myhre, G., Bauer, S. E., Lund, M. T., Karydis, V. A., Kucsera, T. L., Pan, X., Pozzer, A., Skeie, R. B., Steenrod, S. D., Sudo, K., Tsigaridis, K., Tsimpidi, A. P., and Tsyro, S. G.: Investigation of global particulate nitrate from the AeroCom phase III experiment, Atmospheric Chemistry and Physics, 17, 12911-12940, 10.5194/acp-17-12911-2017, 2017.

Cheng, L., Ye, Z., Cheng, S., and Guo, X.: Agricultural ammonia emissions and its impact on PM2.5 concentrations in the Beijing–Tianjin–
190 Hebei region from 2000 to 2018, Environmental Pollution, 291, 118162, https://doi.org/10.1016/j.envpol.2021.118162, 2021.

Dammers, E., McLinden, C. A., Griffin, D., Shephard, M. W., Van Der Graaf, S., Lutsch, E., Schaap, M., Gainairu-Matz, Y., Fioletov, V., Van Damme, M., Whitburn, S., Clarisse, L., Cady-Pereira, K., Clerbaux, C., Coheur, P. F., and Erisman, J. W.: NH3 emissions from large point sources derived from CrIS and IASI satellite observations, Atmos. Chem. Phys., 19, 12261-12293, 10.5194/acp-19-12261-2019, 2019.

Ge, Y., Heal, M. R., Stevenson, D. S., Wind, P., and Vieno, M.: Evaluation of global EMEP MSC-W (rv4.34) WRF (v3.9.1.1) model surface
195 concentrations and wet deposition of reactive N and S with measurements, Geosci. Model Dev., 14, 7021-7046, 10.5194/gmd-14-7021-2021, 2021.

Hauglustaine, D. A., Balkanski, Y., and Schulz, M.: A global model simulation of present and future nitrate aerosols and their direct radiative forcing of climate, Atmospheric Chemistry and Physics, 14, 11031-11063, 10.5194/acp-14-11031-2014, 2014.

Hoesly, R. M., Smith, S. J., Feng, L., Klimont, Z., Janssens-Maenhout, G., Pitkanen, T., Seibert, J. J., Vu, L., Andres, R. J., Bolt, R. M.,
200 Bond, T. C., Dawidowski, L., Kholod, N., Kurokawa, J. I., Li, M., Liu, L., Lu, Z., Moura, M. C. P., O'Rourke, P. R., and Zhang, Q.: Historical (1750–2014) anthropogenic emissions of reactive gases and aerosols from the Community Emissions Data System (CEDS), Geosci. Model Dev., 11, 369-408, 10.5194/gmd-11-369-2018, 2018.

Ianniello, A., Spataro, F., Esposito, G., Allegrini, I., Hu, M., and Zhu, T.: Chemical characteristics of inorganic ammonium salts in PM2.5 in the atmosphere of Beijing (China), Atmos. Chem. Phys., 11, 10803-10822, 10.5194/acp-11-10803-2011, 2011.

205 Szopa, S., Naik V., Adhikary B., Artaxo P., Berntsen T., Collins W.D., Fuzzi S., Gallardo L., Kiendler-Scharr A., Klimont Z., Liao H., Unger N., and P., Z.: Short-Lived Climate Forcers. In Climate Change 2021: The Physical Science Basis. Contribution of Working Group I to the Sixth Assessment Report of the Intergovernmental Panel on Climate Change, Cambridge University Press, Cambridge, United Kingdom and New York, NY, USA, 817-922, 10.1017/9781009157896.008, 2021.

Wang, Y., Zhang, Q. Q., He, K., Zhang, Q., and Chai, L.: Sulfate-nitrate-ammonium aerosols over China: response to 2000–2015 emission
210 changes of sulfur dioxide, nitrogen oxides, and ammonia, Atmos. Chem. Phys., 13, 2635-2652, 10.5194/acp-13-2635-2013, 2013.